# Cell Permeable Stapled Peptide Inhibitor of Wnt Signaling that Targets β-Catenin Protein–Protein Interactions

Laura Dietrich[1,2], Bernd Rathmer[2], Kenneth Ewan[3], Tanja Bange[4], Stefan Heinrichs[5], Trevor C. Dale[3], Dennis Schade[2,6], and Tom N. Grossmann[1,7,8,*]

[1] Chemical Genomics Centre of the Max Planck Society, 44227 Dortmund, Germany

[2] Department of Chemistry and Chemical Biology, TU Dortmund University, 44227 Dortmund, Germany

[3] School of Bioscience, Cardiff University, Cardiff CF10 3AX, United Kingdom

[4] Department of Mechanistic Cell Biology, Max-Planck-Institute of Molecular Physiology, 44227 Dortmund, Germany

[5] Institute for Transfusion Medicine, University Hospital Essen, 45147 Essen, Germany

[6] Institute of Pharmacy, Department of Pharmaceutical & Medicinal Chemistry, University of Greifswald, 17489 Greifswald, Germany

[7] Department of Chemistry and Pharmaceutical Sciences, VU University Amsterdam, 1081 HZ Amsterdam, The Netherlands

[8] Lead Contact

[*] Correspondence: t.n.grossmann@vu.nl

**SUMMARY**

Inhibition of the Wnt signaling pathway is an appealing anti-cancer strategy but most attractive targets are involved in protein–protein interactions (PPIs). Inhibition of such intracellular PPIs is extremely challenging since involved proteins are not accessible for biologics and often lack defined binding pockets complicating the use of small molecules. In principle, peptide-derived modalities hold the potential to bind flat protein surfaces as they are found in PPIs. However, the implementation of robust cellular uptake is complicated which hampers their usefulness. Herein, we investigate the cell penetration properties of a stapled peptide targeting the interaction between β-catenin and TCF/LEF transcription factors which are crucially involved in Wnt signaling. Based on lessons learned from cell-penetrating peptides (CPPs), we design a peptidomimetic with excellent cellular uptake while preserving its affinity for β-catenin. In cell-based assays, this inhibitor shows activity in the low micromolar range exceeding the potency of currently available β-catenin targeting agents.

**KEYWORDS**

Cell-Penetrating Peptides, New Modalities, Peptidomimetics, Protein-Protein Interaction, Wnt Signaling

**INTRODUCTION**

Modified peptides and peptidomimetics represent promising scaffolds for the design of inhibitors of very challenging biological targets. In particular, this involves the inhibition of protein–protein interactions (PPIs) which, due to the absence of addressable pockets, often prove to be reluctant to a targeting by small molecules. Peptides show a propensity to bind flat protein surfaces which are often found in PPI interfaces (Pelay-Gimeno et al. 2015; Qvit et al. 2016). However, most peptides are incapable of passing the cell membrane which limits their usefulness for the inhibition of intracellular targets. Notably, there are exceptions such as cell-penetrating peptides (CPP) which either contain mainly positively charged amino acids (polycationic CPPs, e.g. $R_8$ and Tat) or an alternating pattern of charged and hydrophobic side chains (amphipathic CPPs) (Ziegler 2008). Primary amphipathic peptides are composed of an isolated hydrophobic as well as hydrophilic stretch (e.g. Pep-1). Pep-1 for example consists of a nuclear localization sequence (NLS) contributing positive charges and a hydrophobic tryptophan-rich motif (Morris et al. 2007). Secondary amphipathic peptides on the other hand (e.g. Penetratin) show their amphipathic character only upon adaption of a defined secondary structure (e.g. α-helix) which places hydrophobic and polar residues on opposite sides of the molecule (Deshayes et al. 2011; Eiriksdottir et al. 2010).

Various factors are postulated to support cell surface engagement and penetration of peptides. In general, interactions between positively charged amino acids in CPPs and negatively charged components of the glycocalyx represent the first step towards cellular internalization (Amand et al. 2012; Li et al. 2013). In this respect, arginine proved to be particularly useful (Gasparini et al. 2015; Wender et al. 2008; Wexselblatt et al. 2014). However, charge alone is often insufficient to ensure efficient uptake since charge distribution, secondary structure and hydrophobicity also play important roles. For example, it was shown that macrocyclization of CPPs can improve cellular uptake (Chu et al. 2015; Nischan et al. 2015; Qian et al. 2016; Upadhyaya et al. 2015). Hydrophobicity is integral to amphipathic CPPs and crucial for bilayer insertion and penetration, as hydrophobic amino acids (e.g. tryptophan) interact with the core of membranes (Gallivan et al. 1999; Persson et al. 1998; Regberg et al. 2014; Rydberg et al. 2012). Along those lines, lipidation can also favor the uptake of polar and amphipathic peptides (Lee et al. 2010; Mae et al. 2009; Nelson et al. 2007; Oh et al. 2014). It is important to note that the polar backbone largely contributes to the low cellular uptake of peptides. For that reason, several approaches were pursued to shield backbone amides. That involves N-methylation and the stabilization of certain peptide secondary structures that burry the backbone (Chatterjee et al. 2008; Chatterjee et al. 2013; Pelay-Gimeno et al. 2015). A particularly successful strategy represents the stabilization of α-helices (Azzarito et al. 2013), with hydrocarbon peptide stapling being among the most widely used approaches (Bird et al. 2016; Cromm et al. 2015). Overall, the structural diversity of CPPs complicates the identification of stringent rules that would allow a robust implementation of cell permeability (Brock 2014). This is a tremendous limitation for the design of peptide-derived inhibitors of intracellular proteins.

One particularly challenging intracellular target is β-catenin which regulates the Wnt signaling pathway *via* numerous PPIs. Wnt signaling governs substantial aspects of cell proliferation and differentiation and is involved in the onset and progression of numerous types of cancer. In colorectal cancer for example, hyperactive Wnt signaling occurs in more than 80% of all cases (Chiurillo 2015; Muller et al. 2016). In most adult cells, the Wnt pathway is inactive and β-catenin is constantly degraded by the so-called destruction complex composed of the proteins Adenomatous polyposis coli (APC), Axin, casein kinase 1 (CK1α) and glycogen synthase kinase 3 (GSK3), among others. The destruction complex triggers phosphorylation and subsequent degradation of β-catenin. In healthy cells, activation of Wnt signaling is triggered by diffusible extracellular Wnt proteins which bind to the transmembrane receptor Frizzled (FZD) forming a complex with the low-density lipoprotein receptor-related protein 5/6 (LRP5/6). This leads to the recruitment of Dishevelled (Dvl) and Axin thereby blocking degradation of β-catenin. As a result, β-catenin accumulates and translocates into the nucleus where it triggers the formation of the transactivation complex leading to the transcription of Wnt target genes (Clevers et al. 2012). In an oncogenic context, hyperactivation of Wnt signaling is often triggered by a reduction of destruction complex activity, e.g. *via* mutations in APC, Axin or β-catenin itself, resulting in high levels of β-catenin (Polakis 2012).

Approaches to inhibit Wnt signaling mainly involve the targeting of upstream pathway components: Transmembrane receptors have been inhibited with antibodies and peptidomimetics (Gurney et al. 2012; Jenei et al. 2009; Newnham et al. 2015; Safholm et al. 2008). Small molecules and macrocycles have been used to inhibit the segregation and maturation of Wnt ligands (Chen et al. 2009; Liu et al. 2013; Madan et al. 2016; Proffitt et al. 2013; Xu et al. 2017) and to target enzymes crucial for the function of the destruction complex (Chen et al. 2009; Huang et al. 2009; James et al. 2012; Thorne et al. 2010; Waaler et al. 2012). Since oncogenic mutations often occur in components of the destruction complex which is located in the center of the Wnt pathway, the usefulness of strategies targeting upstream components is limited. Inhibition of the transactivation complex (downstream in the pathway) would be insensitive to such mutations and is therefore considered an appealing anti-cancer strategy (Bertoldo et al. 2016; Emami et al. 2004; Gonsalves et al. 2011). Two stapled peptides have been reported to disrupt intracellular PPIs that involve β-catenin representing a first proof-of-concept (Grossmann et al. 2012; Takada et al. 2012). One of them is StAx (originally named StAx-35R) which targets the interaction between β-catenin and TCF/LEF transcription factors (Grossmann et al. 2012) but suffers from relatively low bioactivity presumably due to low cellular uptake. Herein we describe an integrative strategy to convey robust cellular uptake considering lessons learned from CPPs combined with the utilization of additional hydrophobic and positively charged modalities. This strategy yields a molecule with excellent cellular uptake showing high selectivity for β-catenin and very potent inhibition of proliferation and migration in intestinal cell-based assays.

## RESULTS

### Comparison of cellular uptake

Aiming for the installation of robust cell penetration of stapled peptide StAx, uptake properties of known cell penetrators were compared using five CPPs and one additional stapled peptide (SAHM1, Notch inhibitor (Moellering et al. 2009)). Among the CPPs, polycationic ($Tat_{49-57}$, $R_8$) as well as primary (Pep-1) and secondary (Penetratin) amphipathic sequences were selected (Figure 1A). For the assessment of cellular uptake, we used fluorescently labeled versions (*f-*, fluorescein) of these peptides. It is important to note that the quantitation of uptake is challenging as all established methods suffer from limitations. We decided to avoid techniques that require the fixation of cells as fixation tends to generate false positive results (Richard et al. 2003), and chose a combination of fluorescence confocal microscopy and flow cytometry both employing live cells. Live cell confocal microscopy allows the subcellular localization of peptides but is not quantitative, while flow cytometry is quantitative but does not provide spatial information.

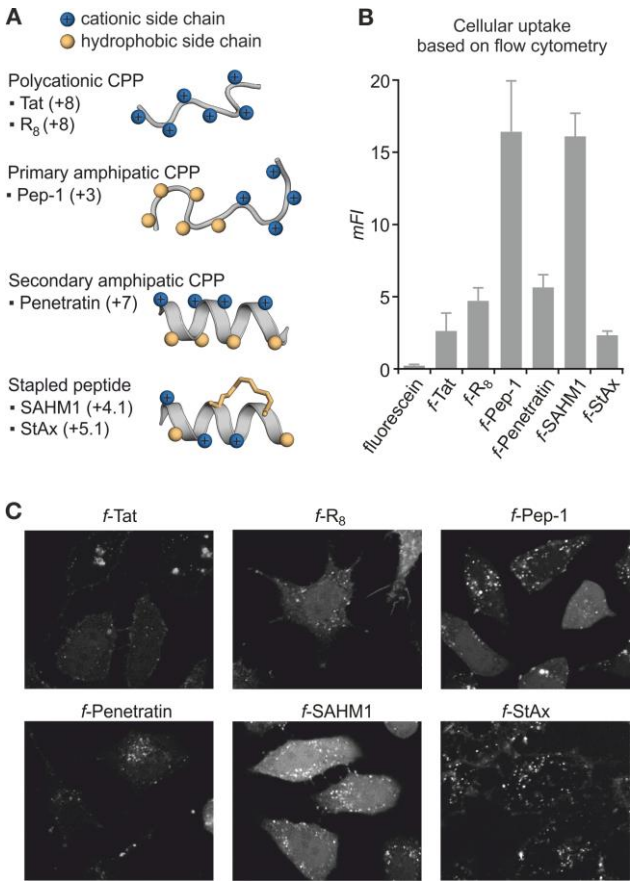


**Figure 1: Cell Permeability of CPPs and Stapled Peptides.** (A) Peptide classes known to penetrate cells including examples (for peptide sequences see Table S2). Net charge of peptides is given (calculated with property calculator by Innovagen AB). (B) Plot of geometric mean fluorescence intensities (mFI) obtained by flow cytometry (10,000 events of live cells, at least three independent biological replicates, error bars represent 1σ). HeLa cells were treated with FITC-labeled peptides (5 µM, 90 min). (C) Live cell confocal fluorescence microscopy of HeLa cells incubated with FITC-labeled peptides (5 µM, 90 min).

For flow cytometry experiments, HeLa cells were incubated with labeled peptides (5 µM, 90 min), then stringently washed and treated with protease to remove cell-surface bound peptides. The mean fluorescence intensity (*mFI*) of analyzed cells reveals for all peptides higher uptake than for the fluorescent label (fluorescein) alone (Figure 1B). Within this panel, primary amphipathic peptide Pep-1 and stapled peptide SAHM1 convey in highest fluorescence intensities, while polycationic peptides (Tat, $R_8$) and secondary amphipathic peptide Penetratin show considerably lower uptake. Interestingly, the uptake of StAx is also in this range and about 7-fold lower than the one of Pep-1 and SAHM1. Using confocal microscopy, we examined the subcellular localization revealing for all peptides (though to a varying extent) cytosolic and nuclear distribution as well as accumulation in intracellular vesicular structures presumably endosomes (Brock 2014) (Figure 1C). SAHM1, Pep-1 and $R_8$ exhibit a comparably high cytosolic fraction while StAx and Penetratin show predominantly vesicular localization. Taken together, stapled peptide SAHM1 and CPP Pep-1 combine cytosolic distribution (microscopy) with high overall uptake (flow cytometry). StAx is only moderately internalized and shows low cytosolic distribution which is similar to the behavior of Tat and Penetratin. Considering StAx' positive net charge (+5.1), stabilized helical conformation and hydrophobic character, it already possesses fundamental features for uptake explaining its basic cell permeability. To increase cellular uptake and ensure robust bioactivity, we applied a strategy that on the one hand aims at fine tuning of core sequence hydrophobicity, and on the other hand explores a variety of *N*-terminal modifications to introduce additional hydrophobic or polar groups.

**Variation of Stapled Peptide StAx**

StAx (Figure 2A) was previously optimized for high target affinity and to incorporate the maximum number of arginines (R) that were compatible with target binding. As a result, there was little potential for additional variations to be made to the core peptide sequence (Figure 2A). Knowing that the six arginine residues in StAx do not significantly contribute to β-catenin binding, we considered the modification of these sites. Since the positively charged guanidinium group is crucial for cell penetration, we focused on the modulation of its alkyl chain aiming at increasing its hydrophobic character, a strategy that has already proven useful for the improvement of CPPs (Wender et al. 2000). For that reason, arginine derivatives with altered linker structures namely homo-arginine (hR, longer alkyl linker) and 4-guanidino-phenylalanine (pR, aromatic linker) were incorporated instead of the natural amino acid (Figure 2B). In the two new resulting peptides, all arginines were replaced either by hR (StAx-h) or by pR (StAx-p). In fluorescence polarization (FP) assays, we verified that peptides *f*-StAx-p and *f*-StAx-h exhibit an affinity for recombinant full length β-catenin ($K_d$ = 66 and 123 nM, respectively) that is in the range of the original StAx peptide ($K_d$ = 108 nM, Figure S1).

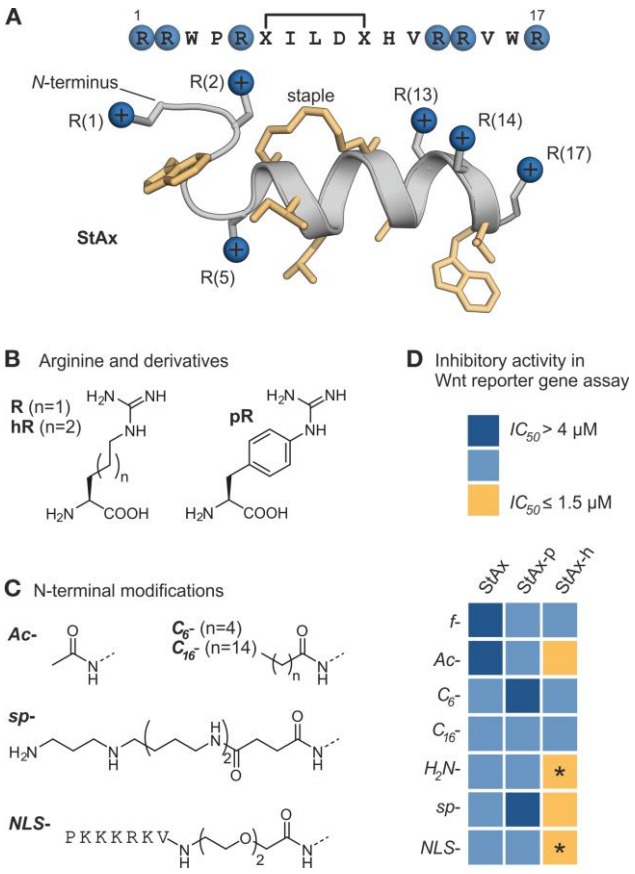


**Figure 2: StAx peptide derivatives inhibit Wnt reporter gene activity.** (A) StAx sequence with schematic representation of its bioactive secondary structure (derived from crystal structure of a related StAx-derivative in complex with β-catenin, PDB: 4DJS). (B) Chemical structure of homo-arginine (hR) and 4-guanidino-phenylalanine (pR). (C) Groups that were employed for N-terminal modification of peptides. (D) Heat map representation of inhibition of Wnt signaling activity (for $IC_{50}$-values see Figure S2) in a Wnt reporter gene assay (293T cells were transfected with: i) Wnt3a-expressing vector, ii) vector with Super (8x)TOPFlash involving TCF-responsive firefly luciferase and iii) vector with *Renilla* luciferase control). After peptide treatment (22 h), luciferase signal was detected (* highest activity within the panel). Experiments were performed at least as two independent biological replicates (each with three technical replicates, for details see STAR Methods and Figure S2).

Based on these three core sequences, we selected a diverse set of N-terminal modifications (Figure 2C). Attachment of different hydrophobic moieties including acetylation (*Ac*-), capronylation ($C_6$) and palmitoylation ($C_{16}$-) stepwise increases hydrophobicity and presumably affinities for membranes. In addition, we investigated hydrophilic modalities involving the free N-terminus ($H_2N$-) and Spermine (*sp*-) as well as the nuclear localization sequence (*NLS*-) of SV40 large T-antigen. This NLS peptide sequence contains four lysines and one arginine (Figure 2C) and was previously used to improve both cellular uptake and nuclear localization (Ragin et al. 2002). The latter is an aspect which may also support biological activity of StAx peptides since the target protein complex is enriched in the nucleus (Cadigan et al. 2012).

The resulting 21 peptides (including fluorescently labeled versions) were synthesized and tested regarding their potential to inhibit canonical Wnt signaling in a cell-based assay. For that purpose, 293T cells were

transfected with two vectors: One with 7 tandem repeats of a TCF/LEF response element (including minimum promoter) upstream of firefly luciferase (TOPflash), and another one with *Renilla* luciferase for normalization (Lanier et al. 2012). Wnt signaling was activated in an autocrine and paracrine fashion by co-transfection with a third vector expressing the Wnt3A ligand. Cells were incubated with varying peptide concentrations (0.1–10 µM) and luciferase activity was measured after 22 h. Corresponding half maximal inhibitory concentrations ($IC_{50}$) were determined. For assay validation, we tested the known Wnt inhibitor XAV939 acting upstream in the signaling pathway which shows inhibition in the expected activity range ($IC_{50}$ = 0.07 µM, Figure S2). Our peptide panel shows diverse inhibitory effects (Figure 2D) but importantly no general toxicity within the tested dose range (based on *Renilla* luciferase). Among the three core sequences, StAx-h harboring six homo-arginine residues shows highest Wnt pathway inhibition. Within the StAx-h series, small and/or hydrophilic modifications result in highest activities with $H_2N$- and *NLS*- being the most active ones ($IC_{50}$ = 1.4 µM).

**StAx-h peptides are efficient cell penetrators**

Knowing that the three core sequences (StAx, StAx-p, StAx-h) show similar affinity for β-catenin (Figure S1), we suspected that differences in inhibitory activity originate from differences in cellular uptake and distribution. To test this hypothesis, cell penetration was investigated by flow cytometry and microscopy employing fluorescently labeled versions of the three core peptides (*f*-StAx, *f*-StAx-p, *f*-StAx-h). In addition, fluorescently labeled NLS-modified StAx-h (*f-NLS*-StAx-h) was included as it showed highest activity in the reporter gene assay (together with $H_2N$-StAx-h). Flow cytometry-based readout of cellular uptake was performed using a dilution series of peptides (0.1–5 µM, 90 min, Figure 3A). Overall, uptake increases with peptide concentration (though to a varying extent) with all variants showing improved penetration when compared to the original StAx peptide (black). Interestingly, *f-NLS*-StAx-h exhibits the largest increase (7-fold at 5 µM) with respect to StAx placing it in the range of the best CPPs (*mFI* at 5 µM: 17.0 for *f*-NLS-StAx-h, 16.4 for Pep-1, Figure 1B). Subsequently, life cell confocal microscopy was performed (5 µM, 90 min, Figure 3B) to investigate the subcellular localization of all four peptides. Peptide *f*-StAx-p is predominantly membrane associated (Figure 3B) presumably do the strong hydrophobic character of the aromatic moiety in pR. In contrast, the two StAx-h derivatives show considerable cytosolic distribution which is particularly pronounced for *f-NLS*-StAx-h (Figure 3B).

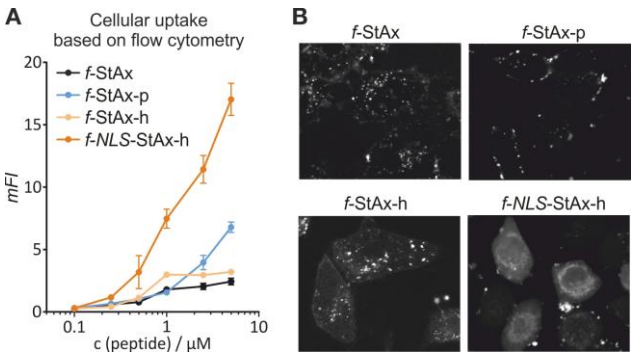


**Figure 3: Cellular Uptake of selected StAx peptides.** (A) Plot of geometric mean fluorescence intensities (mFI) obtained by flow cytometry (10,000 events of live cells, at least three independent biological replicates, error bars represent 1σ). HeLa cells were treated with fluorescently-labeled peptides (0.1–5 µM, 90 min). (B) Live cell confocal fluorescence microscopy depicting HeLa cells incubated with fluorescently-labeled peptides (5 µM, 90 min). For details see STAR Methods.

### StAx-h binds β-catenin and inhibits Wnt target gene expression

Taken together, Wnt reporter activity (Figure 2D) and cell permeability (Figure 3) indicate that core sequence StAx-h holds the highest potential for efficient inhibition of Wnt signaling. Before investigating StAx-h potency in detail, we aimed for the validation of its binding to β-catenin in a cellular context. For that purpose, pull-down experiments were performed using a biotinylated version of StAx-h (*b*-StAx-h). The peptide was immobilized on Streptavidin beads and incubated with the lysate of DLD-1 cells, a colon cancer cell line with elevated β-catenin levels. After stringent washing, bound proteins were subjected to tryptic digestion and fragments analyzed by HPLC-coupled high-resolution mass spectrometry. Identified proteins were plotted in accordance to their enrichment and statistical relevance compared to pull-down with beads only. The resulting volcano plot (Figure 4A) shows 37 proteins that are significantly enriched with β-catenin being one of the highest scoring ones (orange, Figure 4A). Most strikingly, among the remaining 36 proteins, 17 are proposed components of β-catenin containing complexes (blue, Figure 4A, for complete list see Table S3) supporting selective binding of StAx-h to β-catenin. Most of these potential complex partners are either involved in transcriptional activator complexes (e.g. RUVBL1 and RUVBL2) or cell-cell adhesion junctions (e.g. α-catenin and E-cadherin).

Having verified StAx-h as β-catenin binder, we investigated its effects on the expression of Wnt target genes using mouse-derived small intestinal crypt organoids expressing a doxycycline(dox)-inducible and stable form of β-catenin (activated β-catenin) (Dale et al. 2015; Jarde et al. 2013). Importantly, removal of dox (-dox, Figure 4B) results in loss of activated β-catenin thereby reducing the mRNA level of Wnt target genes (e.g. *Axin2*, *Myc*, *Ascl2*, *Tiam1*) and increasing levels of differentiation marker Car4. Notably, treatment with $H_2N$-StAx-h (Figure S3) or *NLS*-StAx-h (Figure 4B) results in gene expression changes consistent with

inhibition of Wnt signaling following loss of activated β-catenin resulting from doxycycline removal (–dox, Figure 4B). For *NLS*-StAx-h, this effect is observed as early as 2 h after initiation of treatment and plateaus after ca. 6 h with mRNA levels in the range of the control sample lacking activated β-catenin expression. As an additional control, StAx-h-derived peptide StCo (for sequence see Table S2) was designed that shows greatly diminished affinity for β-catenin ($K_d$ ~ 10 µM, Figure S1) due to the substitution of three amino acids directly involved in β-catenin binding. Importantly, the NLS-modified version of this peptide (*NLS*-StCo) does not alter the level of investigated Wnt-responsive target genes (Figure 4B).

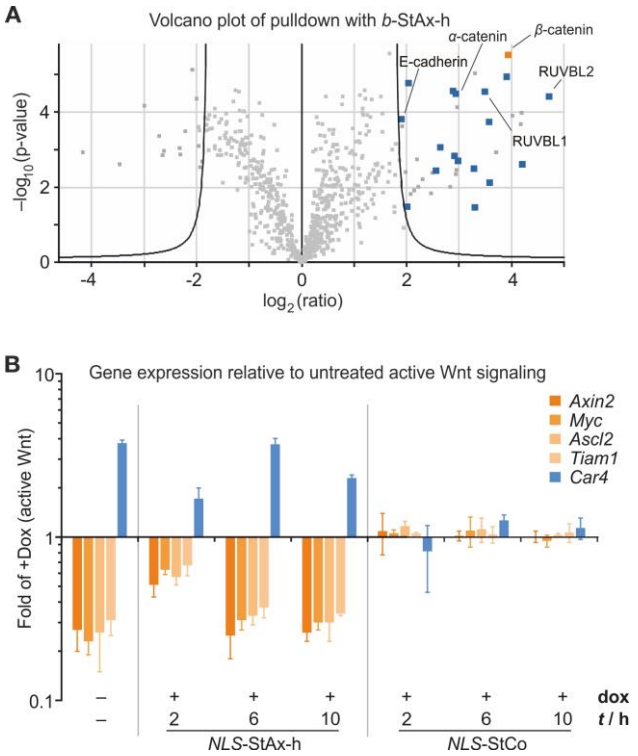


**Figure 4: Wnt-pathway selectivity of StAx-h peptides.** (A) Volcano plot of pull-down with biotinylated StAx-h (*b*-StAx-h) which was immobilized on streptavidin-coated beads and incubated with DLD-1 cell lysate (3 h). β-catenin (orange) and significantly enriched known binding partners in β-catenin-containing complexes (blue) are highlighted (for complete list of pull-down results see Table S3). (B) Target gene expression in small intestinal colon crypt organoids expressing a dox-inducible mutant β-catenin (Tet-O-Δ1-89-β-catenin). Level are plotted relative to dox-induced cells (+dox) lacking peptide treatment. Organoids induced with 4 µg/mL dox were treated with 10 µM *NLS*-StAx-h or *NLS*-StCo (for sequence see Table S2). mRNA level of Wnt target genes (*Myc*, *Ascl2*, *Tiam1* or *Axin2*), and of differentiation marker *Car4* were quantified. Gene expression changes as a result of removal of dox for the last 24 h (–dox) are shown on the left. Experiments were performed as three independent biological replicates, each with three technical replicates. Values in all bar graphics depict mean values and error bars represent 1σ. *$p < 0.05$, ns = not significant.

***NLS*-StAx-h Inhibits Proliferation and Migration of Colorectal Cancer Cells**

Inhibition of Wnt signaling reduces growth of Wnt-dependent cancer cell lines but has no effect on cells that grow independent of Wnt signaling. To test activity and specificity of StAx-h peptides, cancer cell lines originating from different human tissues were screened for their sensitivity towards inhibitor treatment. This involves Wnt-addicted colon cancer cell lines DLD-1 and SW-480 in which the Wnt-pathway is activated *via* truncations of the destruction complex component APC. In addition, we chose cell lines that are reported to be Wnt-independent: U87 glioblastoma cells, MCF-7 breast cancer cells and U2OS osteosarcoma cells (Forbes et al. 2015). Viability read-out was performed *via* quantitation of cellular ATP levels. Compared to previous studies, inhibitors ($c$ = 10 µM) were tested under stringent conditions using normal serum concentration (rather than starving conditions) (Huang et al. 2009) and a relatively short incubation time of 72 h (compared to 5–6 d) (Chen et al. 2009; Fujii et al. 2007; Grossmann et al. 2012). Under these conditions, original peptide *Ac*-StAx and known Axin stabilizer XAV939 do not show significant effects on the viability of Wnt-addicted DLD-1 and SW-480 cells. The two peptides performing best in the reporter gene assay ($H_2N$-StAx-h and *NLS*-StAx-h) were also tested. $H_2N$-StAx-h only shows a moderate effect on SW-480 cells (38 % inhibition) while most cell penetrating stapled peptide *NLS*-StAx-h reduces viability of both SW-480 and DLD-1 by more than 80 % (Figure 5A). Control peptide *NLS*-StCo, lacking affinity for β-catenin, does not have an effect on viability. As expected, none of the StAx-derived peptides inhibits growth of Wnt-independent cell lines (U87, U2OS and MCF7, Figure 5A). Interestingly, XAV939 shows some effect on the viability of MFC7 cells (48 % inhibition) indicating some activity that is independent from inhibition of Wnt signaling.

Having studied the cellular uptake of fluorescently labeled StAx-derivatives in detail, we also tested their effect on viability (Figure S4). In line with the reporter gene assay and its relatively low cellular uptake, *f*-StAx-h shows very low activity on Wnt-dependent SW-480 cells. For *f-NLS*-StAx-h, we observe activity in the range of the non-labeled version indicating comparable cellular uptake. Interestingly, both fluorescently labeled peptides (*f*-StAx-h and *f-NLS*-StAx-h) cause ca. 20% reduction of viability for Wnt-independent MFC-7 cells (Figure S4) indicating non-specific toxicity caused by the fluorescein label. Notably, the most active peptide (*NLS*-StAx-h) harbors a nuclear localization signal which apparently does not result in nuclear accumulation (Figure 3B). For that reason, we were interested if its high cellular activity is predominantly caused by high cellular uptake due to the five positively charged NLS side chains. For that purpose, a charge analog harboring five N-terminal lysine residues instead of the NLS (*KKKKK*-StAx-h) was designed. And indeed, *KKKKK*-StAx-h reduces the viability of Wnt-addicted SW-480 similar to *NLS*-StAx-h while not affecting Wnt-independent MCF-7 cells. In line with this observation, the overall cellular uptake of *f-KKKKK*-StAx-h is

only slightly lower than that of *f-NLS*-StAx-h (*mFI* at 5 µM: 13.9 vs. 17.0, Figure S5) indicating that the high cellular activity of the NLS-modified version is mainly triggered by increased cellular uptake supported by positive charges within the NLS.

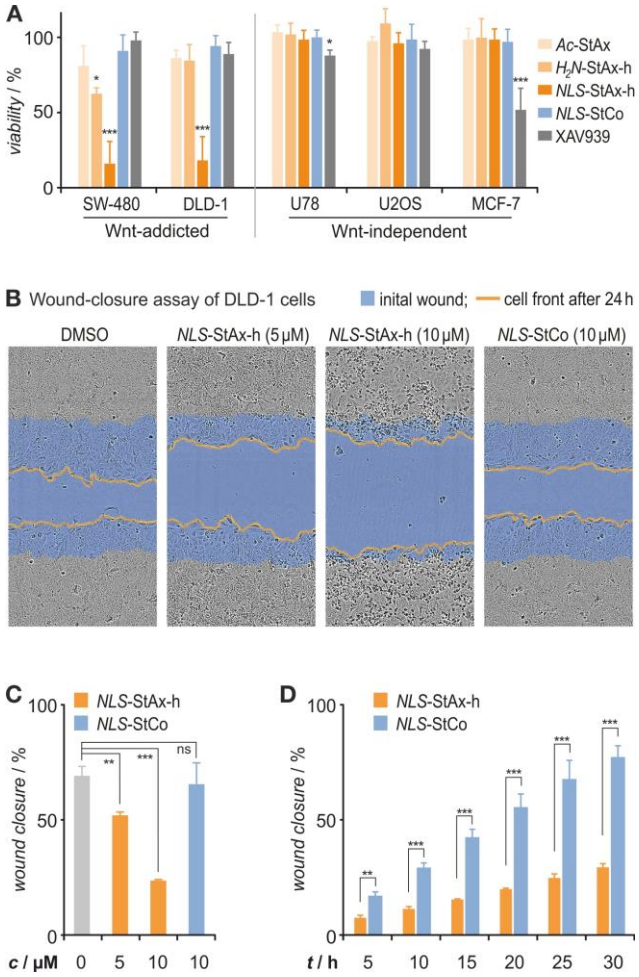


**Figure 5: *NLS*-StAx-h inhibits cell proliferation and migration.** (A) Viability assay of Wnt-addicted (SW-480, DLD-1) and Wnt-independent cell lines (U87, U2OS, MCF-7) after treatment with compound (10 µM, 72 h). Viability is plotted relative to DMSO treated cells. (B) Wound-closure assay of DLD-1 cells. For 24 h, cells were treated with either DMSO or peptide at given concentration (grey: initial cell area, blue: initial wound, orange line: front of cells after 24 h. (C) Wound closure of experiment in Figure 5B was quantified. Experiments were performed as three independent biological replicates, each with three technical replicates. (D) Time-dependent wound-closure assay comparing treatment with *NLS*-StAx-h (orange) and control peptide *NLS*-StCo (blue). Experiments were performed as three independent biological replicates, each with three technical replicates. Values in all bar graphics depict mean values and error bars represent 1σ. *$p < 0.05$, **$p < 0.01$, ***$p < 0.001$, ns = not significant).

The active Wnt pathway not only supports cell proliferation, but also cell migration which crucially contributes to cancer metastasis (Iskit et al. 2015; Li et al. 2011; Sack et al. 2011). Thus, most active peptide

*NLS*-StAx-h and control peptide *NLS*-StCo were tested in a wound-closure assay using DLD-1 cells. After introduction of a sterile wound (blue, Figure 5B), cells were treated either with DMSO or with one of the peptides for 24 h. In absence of peptide (DMSO), the original wound was already closed by 69 % after 24 h, while *NLS*-StAx-h treatment resulted in dose-dependent inhibition of this process (wound closure: 52 % at 5 µM, and 24 % at 10 µM, Figure 5B and C). As expected, *NLS*-StCo (10 µM) shows no inhibitory effect. This robust inhibition of cell migration, was confirmed by time-dependent measurements (Figure 5D) revealing significant inhibition of wound-closure as early as 5 h after initiation of treatment. As an additional control, we performed the wound-closure assay with Wnt-independent MCF-7 cells. Importantly, these cells were not affected by *NLS*-StAx-h treatment (Figure S6). Together with the inactivity of control peptide *NLS*-StCo, this indicates that indeed Wnt-inhibition is responsible for observed effects on the migration of DLD-1 cells.

**DISCUSSION**

Previously we reported a stapled peptide (StAx) that targets β-catenin, the central hub in canonical Wnt-signaling, but its activity suffers from low cellular uptake. Even though there is some rational, it is not possible to design highly cell permeable and bioactive stapled peptides from scratch (Bird et al. 2016; Chu et al. 2015; Cromm et al. 2016). It is known that some features appear to be necessary (but not sufficient) for efficient uptake of positively charged peptides: (a) A certain degree of hydrophobicity, and (b) A spatially separated hydrophobic and cationic stretch. Presumably, this is due to a two-step uptake mechanism that initially involves interaction of cationic peptide groups with negatively charged membrane components which is followed by insertion of hydrophobic residues into the membrane core.

To evaluate cell permeability of StAx, we compared its cellular uptake and localization with known CPPs (5 µM, 90 min, HeLa cells). Interestingly, StAx uptake is in the range of first generation CPPs such as Tat but about 7-times lower than best performing peptides Pep-1 and SAHM1. StAx already has a number of hydrophobic and positively charged amino acids, however, they are spatially not separated. Since there is only little room for a variation of the StAx core sequence, we decided to pursue a strategy that considers minor sequence alterations (derivatization of existing arginines) and a set of hydrophobic and polar *N*-terminal modifications (including an NLS). At this point, it was not clear whether uptake would be supported by additional cationic or hydrophobic groups. After validating that arginine derivatization does not interfere with β-catenin binding, a small library consisting of 21 modified peptides was synthesized and tested regarding their activity in a Wnt-dependent reporter gene assay. This assay showed that polar *N*-terminal modifications in combination with a slightly more hydrophobic core sequence (homo-arginine instead of arginine) provide most active peptides. While activity trends observed for the reporter gene assay are in line with growth inhibition, the dynamic range in the reporter gene assay is smaller. This behavior can be due to the non-physiological concentration and activity of the promotor used in the reporter gene assay, and it highlights the importance of more relevant secondary cell-based assays for hit validation. Analysis of cell permeability revealed that in particular the analogue with an N-terminal NLS sequence (*NLS*-StAx-h) shows very high cellular uptake and cytosolic distribution comparable to best cell penetrators Pep-1 and SAHM1. Interestingly, a charge analog bearing five lysine residues instead of the NLS shows similar cellular uptake indicating that the basic character of the NLS is of central importance.

Having an active and cell permeable peptide available, we were interested if the peptide indeed targets β-catenin in a cellular context. To address this question, pull-down experiments were performed using a biotinylated StAx-h peptide and analyzed with high-resolution MS. In this assay, β-catenin and some of its

known binding partners were significantly enriched verifying β-catenin binding. Notably, we did not identify any of the LEF/TCF transcription factors which is expected since they compete with StAx-h for β-catenin binding. Analysis of changes in the transcription of Wnt-target genes in mouse-derived small intestinal crypts unambiguously shows inhibition of Wnt signaling after treatment with StAx-h. Importantly, an *NLS*-StAx-h derived control peptide (*NLS*-StCo) does not affect mRNA level of these genes.

In a number of cancer cells types, expression of Wnt-target genes is essential for cell proliferation and migration which are crucial for the oncogenicity of these cells. Consequently, selective inhibition of Wnt-signaling is considered an appealing anti-cancer strategy. In this respect, it is important to note that oncogenic mutations that lead to hyperactive Wnt-signaling are often found downstream (right Figure 6), i.e. at the level of the destruction complex (e.g. in APC) or in β-catenin itself. For that reason, inhibitors that act on upstream pathway components involved in Wnt biosynthesis, membrane signal transduction or regulation of the destruction complex (left, Figure 6) are of limited therapeutic use in such a context. This renders inhibitors of the downstream interaction between β-catenin and LEF/TCF transcription factors, such as *NLS*-StAx-h, interesting tool compounds to test the potential of this targeting strategy.

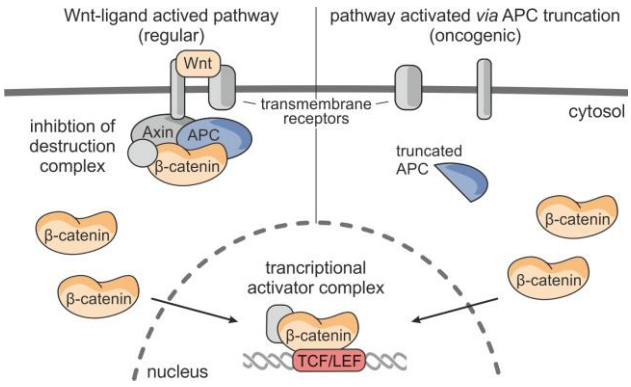


**Figure 6: Oncogenic activation of Wnt signaling via APC truncation.** Schematic representation of the Wnt pathway activated either regularly *via* diffusible Wnt ligands (left), or oncogenically *via* truncation of APC (right).

To investigate the potency and specificity of *NLS*-StAx-h, we tested its impact on the viability of Wnt-dependent and -independent cell lines. Applying stringent assay conditions (high serum concentration and relatively short incubation times), we observed inhibition of proliferation (80% inhibition after 72 h) and migration (2.8-fold reduced wound-closure after 24 h) only for Wnt-dependent cell lines. Importantly, activity of *NLS*-StAx-h exceeds that of known Wnt inhibitor XAV939 which stabilizes a component of the destruction complex and does not show inhibition of cell proliferation under our stringent conditions. The same holds true for starting peptide StAx which highlights the importance of robust cellular uptake for high

activity. Interestingly, published small molecule inhibitors of downstream Wnt-signaling are required to be applied at higher concentrations (iCRT3: 75 µM, ICG-001: 25µM vs. *NLS*-StAx-h: 10 µM) to interfere with cell proliferation (Emami et al. 2004; Gonsalves et al. 2011). Given the inherent difficulties associated with peptide uptake, this is highly remarkable and highlights the significance of our optimization strategy as well as the importance of *NLS*-StAx-h for the future investigation of approaches that target the Wnt transactivation complex.

**SIGNIFICANCE**

The development of highly cell permeable and bioactive peptides is extremely challenging and represents the bottleneck for an application of peptide-derived molecules. The strategy reported herein allowed the implementation of robust cell permeability using a stapled peptide with low cellular uptake as starting point. Importantly, this approach should be applicable to a multitude of peptide-derived inhibitors that suffer from low uptake. Herein described stapled peptide *NLS*-StAx-h inhibits oncogenic Wnt signaling which is a driver in numerous types of cancer, in particular in colorectal cancer (CRC). CRC is the third most common cancer in men and the second most common cancer in women. The overall survival rate is as low as 8.5% and highlights the need for novel and efficient therapies. Aiming for the inhibition of intracellular pathway components, small molecules have been developed mainly targeting enzymes that are involved in multiple signaling pathways which holds the risk of undesired side effects. The development of novel targeting strategies is complicated since Wnt signaling is regulated by numerous PPIs which proved reluctant to inhibition by small molecules. *NLS*-StAx-h inhibits the interaction between β-catenin and corresponding transcription factors targeting the very end of the Wnt pathway. Importantly, this is the first compound that combines good cellular uptake with efficient inhibition of β-catenin–transcription factor interactions. These features render *NLS*-StAx-h an extremely potent and selective Wnt inhibitor thereby providing a highly valuable pharmacological tool for the investigation of a targeting approach that acts on downstream components of the pathway for cancer treatment.

**STAR METHODS**

Detailed methods are provided in the online version of this paper and include the following:

- KEY RESOURCES TABLE
- CONTACT FOR REAGENT AND RESOURCE SHARING
- EXPERIMENTAL MODEL AND SUBJECT DETAILS
    - Bacterial Strains
    - Cell Lines
    - Mice
- METHODS DETAILS
    - Peptide Synthesis
    - β-catenin Expression and Purification
    - Fluorescence Polarization Assay
    - Flow Cytometry
    - Confocal Microscopy
    - Dual Luciferase Reporter Gene Assay
    - Pull-Down Assay
    - Mass Spectrometry of Pull-Down Assay
    - qRT-PCR from Small Intestinal Crypt Organoids
    - Viability Assay
    - Wound-Closure Assay
- QUANTIFICATION AND STATISTICAL ANALYSIS

**AUTHOR CONTRIBUTIONS**

L.D. and T.N.G. designed the study; L.D. generated peptides, performed microscopy and cytometry-based peptide-uptake studies, executed in vitro binding and pull-down assays as well as cell-based viability and cell migration assays; S.H. supported conductance and analysis of peptide uptake assays. B.R. performed and evaluated peptides in Wnt reporter gene assay with support from D.S. T.B. supported the pull-down assay and performed MS-based analysis. K.E. conducted ex vivo colon crypt organoid assay with support from T.C.D. L.D., B.R., K.E., and T.B. analyzed the data; L.D. and T.N.G. wrote the manuscript, which was reviewed by all co-authors.

**ACKNOWLEDGEMENTS**

We are grateful for support from AstraZeneca, Bayer CropScience, Bayer HealthCare, Boehringer Ingelheim, Merck KGaA and the Max Planck Society. T.N.G. thanks the Deutsche Forschungsgemeinschaft (DFG; Emmy Noether program GR3592/2-1) and the European Reasearch Council (ERC; ERC starting grant, no. 678623). D.S. acknowledges financial support by the German Federal Ministry of Education and Research (BMBF, grant 131605). We thank S. Gentz, K. Kuhr and F. Müller for technical assistance with peptide synthesis, high-resolution mass spectrometry and pull-down assays, respectively.

**SUPPORTING CITATION**

The following references appear in the Supplemental Information:

(Bauer et al. 2000; Bol et al. 2015; Chen et al. 2015; Chen et al. 2014; Choi et al. 2009; Conaway et al. 2011; Cruciat et al. 2013; Gareau et al. 2012; Guo et al. 2014; Havugimana et al. 2012; Hou et al. 2006; Huber et al. 2001; Jamieson et al. 2014; Kawajiri et al. 2009; Kerr et al. 2011; Kim et al. 2006; Kim et al. 2007; Kowalczyk et al. 1997; Krois et al. 2016; Lee et al. 2006; Low et al. 2014; Miller et al. 2012; Mosimann et al. 2009; Pokutta et al. 2000; Sadot et al. 2001; Sato et al. 2005; Shitashige et al. 2008; Tian et al. 2004)

**REFERENCES**

Amand, H. L., Rydberg, H. A., Fornander, L. H., Lincoln, P., Norden, B.and Esbjorner, E. K. (2012). Cell surface binding and uptake of arginine- and lysine-rich penetratin peptides in absence and presence of proteoglycans. Biochim Biophys Acta, *1818***,** 2669-2678.

Azzarito, V., Long, K., Murphy, N. S.and Wilson, A. J. (2013). Inhibition of alpha-helix-mediated protein-protein interactions using designed molecules. Nat Chem, *5***,** 161-173.

Bauer, A., Chauvet, S., Huber, O., Usseglio, F., Rothbacher, U., Aragnol, D., Kemler, R.and Pradel, J. (2000). Pontin52 and reptin52 function as antagonistic regulators of beta-catenin signalling activity. EMBO J, *19***,** 6121-6130.

Bertoldo, D., Khan, M. M., Dessen, P., Held, W., Huelsken, J.and Heinis, C. (2016). Phage Selection of Peptide Macrocycles against beta-Catenin To Interfere with Wnt Signaling. ChemMedChem, *11***,** 834-839.

Bird, G. H., Mazzola, E., Opoku-Nsiah, K., Lammert, M. A., Godes, M., Neuberg, D. S.and Walensky, L. D. (2016). Biophysical determinants for cellular uptake of hydrocarbon-stapled peptide helices. Nat Chem Biol, *12***,** 845-852.

Bol, G. M., Vesuna, F., Xie, M., Zeng, J., Aziz, K., Gandhi, N., Levine, A., Irving, A., Korz, D., Tantravedi, S., et al. (2015). Targeting DDX3 with a small molecule inhibitor for lung cancer therapy. EMBO Mol Med, *7***,** 648-669.

Brock, R. (2014). The uptake of arginine-rich cell-penetrating peptides: putting the puzzle together. Bioconjug Chem, *25***,** 863-868.

Cadigan, K. M.and Waterman, M. L. (2012). TCF/LEFs and Wnt signaling in the nucleus. Cold Spring Harb Perspect Biol, *4*.

Chatterjee, J., Gilon, C., Hoffman, A.and Kessler, H. (2008). N-methylation of peptides: a new perspective in medicinal chemistry. Acc Chem Res, *41***,** 1331-1342.

Chatterjee, J., Rechenmacher, F.and Kessler, H. (2013). N-methylation of peptides and proteins: an important element for modulating biological functions. Angew Chem Int Ed Engl, *52***,** 254-269.

Chen, B., Dodge, M. E., Tang, W., Lu, J., Ma, Z., Fan, C. W., Wei, S., Hao, W., Kilgore, J., Williams, N. S., et al. (2009). Small molecule-mediated disruption of Wnt-dependent signaling in tissue regeneration and cancer. Nat Chem Biol, *5***,** 100-107.

Chen, H. H., Yu, H. I., Cho, W. C.and Tarn, W. Y. (2015). DDX3 modulates cell adhesion and motility and cancer cell metastasis via Rac1-mediated signaling pathway. Oncogene, *34***,** 2790-2800.

Chen, T., Lin, K., Chen, C., Lee, S., Lee, P., Liu, Y., Kuo, Y., Wang, F., Lai, J.and Huang, C. F. (2014). Using an in Situ Proximity Ligation Assay to Systematically Profile Endogenous Protein-Protein Interactions in a Pathway Network. J. Proteome Res., *13***,** 5339-5346.

Chiurillo, M. A. (2015). Role of the Wnt/beta-catenin pathway in gastric cancer: An in-depth literature review. World J Exp Med, *5***,** 84-102.

Choi, H. J., Gross, J. C., Pokutta, S.and Weis, W. I. (2009). Interactions of plakoglobin and beta-catenin with desmosomal cadherins: basis of selective exclusion of alpha- and beta-catenin from desmosomes. J Biol Chem, *284***,** 31776-31788.

Chu, Q., Moellering, R. E., Hilinski, G. J., Kim, Y. W., Grossmann, T. N., Yeh, J. T.and Verdine, G. L. (2015). Towards understanding cell penetration by stapled peptides. Med.Chem.Comm., *6***,** 111-119.

Clevers, H.and Nusse, R. (2012). Wnt/beta-catenin signaling and disease. Cell, *149***,** 1192-1205.

Conaway, R. C.and Conaway, J. W. (2011). Function and regulation of the Mediator complex. Curr Opin Genet Dev, *21***,** 225-230.

Cox, J., Hein, M. Y., Luber, C. A., Paron, I., Nagaraj, N.and Mann, M. (2014). Accurate proteome-wide label-free quantification by delayed normalization and maximal peptide ratio extraction, termed MaxLFQ. Mol Cell Proteomics, *13***,** 2513-2526.

Cox, J.and Mann, M. (2008). MaxQuant enables high peptide identification rates, individualized p.p.b.-range mass accuracies and proteome-wide protein quantification. Nat Biotechnol, *26***,** 1367-1372.

Cromm, P. M., Spiegel, J.and Grossmann, T. N. (2015). Hydrocarbon stapled peptides as modulators of biological function. ACS Chem Biol, *10***,** 1362-1375.

Cromm, P. M., Spiegel, J., Kuchler, P., Dietrich, L., Kriegesmann, J., Wendt, M., Goody, R. S., Waldmann, H.and Grossmann, T. N. (2016). Protease-Resistant and Cell-Permeable Double-Stapled Peptides Targeting the Rab8a GTPase. ACS Chem Biol, *11***,** 2375-2382.

Cruciat, C. M., Dolde, C., De Groot, R. E., Ohkawara, B., Reinhard, C., Korswagen, H. C.and Niehrs, C. (2013). RNA helicase DDX3 is a regulatory subunit of casein kinase 1 in Wnt-beta-catenin signaling. Science, *339***,** 1436-1441.

Dale, T., Clarke, P. A., Esdar, C., Waalboer, D., Adeniji-Popoola, O., Ortiz-Ruiz, M. J., Mallinger, A., Samant, R. S., Czodrowski, P., Musil, D., et al. (2015). A selective chemical probe for exploring the role of CDK8 and CDK19 in human disease. Nat Chem Biol, *11***,** 973-980.

Deshayes, S., Konate, K., Aldrian, G., Heitz, F.and Divita, G. (2011). Interactions of amphipathic CPPs with model membranes. Methods Mol Biol, *683***,** 41-56.

Eiriksdottir, E., Konate, K., Langel, U., Divita, G.and Deshayes, S. (2010). Secondary structure of cell-penetrating peptides controls membrane interaction and insertion. Biochim Biophys Acta, *1798***,** 1119-1128.

Emami, K. H., Nguyen, C., Ma, H., Kim, D. H., Jeong, K. W., Eguchi, M., Moon, R. T., Teo, J. L., Kim, H. Y., Moon, S. H., et al. (2004). A small molecule inhibitor of beta-catenin/CREB-binding protein transcription [corrected]. Proc Natl Acad Sci U S A, *101***,** 12682-12687.

Forbes, S. A., Beare, D., Gunasekaran, P., Leung, K., Bindal, N., Boutselakis, H., Ding, M., Bamford, S., Cole, C., Ward, S., et al. (2015). COSMIC: exploring the world's knowledge of somatic mutations in human cancer. Nucleic Acids Res, *43***,** D805-811.

Fujii, N., You, L., Xu, Z., Uematsu, K., Shan, J., He, B., Mikami, I., Edmondson, L. R., Neale, G., Zheng, J., et al. (2007). An antagonist of dishevelled protein-protein interaction suppresses beta-catenin-dependent tumor cell growth. Cancer Res, *67***,** 573-579.

Gallivan, J. P.and Dougherty, D. A. (1999). Cation-pi interactions in structural biology. Proc Natl Acad Sci U S A, *96***,** 9459-9464.

Gareau, J. R., Reverter, D.and Lima, C. D. (2012). Determinants of small ubiquitin-like modifier 1 (SUMO1) protein specificity, E3 ligase, and SUMO-RanGAP1 binding activities of nucleoporin RanBP2. J Biol Chem, *287***,** 4740-4751.

Gasparini, G., Bang, E. K., Montenegro, J.and Matile, S. (2015). Cellular uptake: lessons from supramolecular organic chemistry. Chem Commun (Camb), *51***,** 10389-10402.

Gonsalves, F. C., Klein, K., Carson, B. B., Katz, S., Ekas, L. A., Evans, S., Nagourney, R., Cardozo, T., Brown, A. M.and Dasgupta, R. (2011). An RNAi-based chemical genetic screen identifies three small-molecule inhibitors of the Wnt/wingless signaling pathway. Proc Natl Acad Sci U S A, *108***,** 5954-5963.

Grossmann, T. N., Yeh, J. T., Bowman, B. R., Chu, Q., Moellering, R. E.and Verdine, G. L. (2012). Inhibition of oncogenic Wnt signaling through direct targeting of beta-catenin. Proc Natl Acad Sci U S A, *109***,** 17942-17947.

Guo, Z., Neilson, L. J., Zhong, H., Murray, P. S., Zanivan, S.and Zaidel-Bar, R. (2014). E-cadherin interactome complexity and robustness resolved by quantitative proteomics. Sci Signal, *7***,** rs7.

Gurney, A., Axelrod, F., Bond, C. J., Cain, J., Chartier, C., Donigan, L., Fischer, M., Chaudhari, A., Ji, M., Kapoun, A. M., et al. (2012). Wnt pathway inhibition via the targeting of Frizzled receptors results in decreased growth and tumorigenicity of human tumors. Proc Natl Acad Sci U S A, *109***,** 11717-11722.

Havugimana, P. C., Hart, G. T., Nepusz, T., Yang, H., Turinsky, A. L., Li, Z., Wang, P. I., Boutz, D. R., Fong, V., Phanse, S., et al. (2012). A census of human soluble protein complexes. Cell, *150***,** 1068-1081.

Hou, R., Liu, L., Anees, S., Hiroyasu, S.and Sibinga, N. E. (2006). The Fat1 cadherin integrates vascular smooth muscle cell growth and migration signals. J Cell Biol, *173***,** 417-429.

Huang, S. M., Mishina, Y. M., Liu, S., Cheung, A., Stegmeier, F., Michaud, G. A., Charlat, O., Wiellette, E., Zhang, Y., Wiessner, S., et al. (2009). Tankyrase inhibition stabilizes axin and antagonizes Wnt signalling. Nature, *461***,** 614-620.

Huber, A. H.and Weis, W. I. (2001). The structure of the beta-catenin/E-cadherin complex and the molecular basis of diverse ligand recognition by beta-catenin. Cell, *105***,** 391-402.

Hubner, N. C.and Mann, M. (2011). Extracting gene function from protein-protein interactions using Quantitative BAC InteraCtomics (QUBIC). Methods, *53***,** 453-459.

Iskit, S., Schlicker, A., Wessels, L.and Peep, D. S. (2015). Fra-1 is a key driver of colon cancer metastasis and a Fra-1 classifier predicts disease-free survival. Oncotarget, *6***,** 43146-43161.

James, R. G., Davidson, K. C., Bosch, K. A., Biechele, T. L., Robin, N. C., Taylor, R. J., Major, M. B., Camp, N. D., Fowler, K., Martins, T. J., et al. (2012). WIKI4, a novel inhibitor of tankyrase and Wnt/ss-catenin signaling. PLoS One, *7*, e50457.

Jamieson, C., Sharma, M.and Henderson, B. R. (2014). Targeting the beta-catenin nuclear transport pathway in cancer. Semin Cancer Biol, *27*, 20-29.

Jarde, T., Evans, R. J., Mcquillan, K. L., Parry, L., Feng, G. J., Alvares, B., Clarke, A. R.and Dale, T. C. (2013). In vivo and in vitro models for the therapeutic targeting of Wnt signaling using a Tet-ODeltaN89beta-catenin system. Oncogene, *32*, 883-893.

Jenei, V., Sherwood, V., Howlin, J., Linnskog, R., Safholm, A., Axelsson, L.and Andersson, T. (2009). A t-butyloxycarbonyl-modified Wnt5a-derived hexapeptide functions as a potent antagonist of Wnt5a-dependent melanoma cell invasion. Proc Natl Acad Sci U S A, *106*, 19473-19478.

Kawajiri, K., Kobayashi, Y., Ohtake, F., Ikuta, T., Matsushima, Y., Mimura, J., Pettersson, S., Pollenz, R. S., Sakaki, T., Hirokawa, T., et al. (2009). Aryl hydrocarbon receptor suppresses intestinal carcinogenesis in ApcMin/+ mice with natural ligands. Proc Natl Acad Sci U S A, *106*, 13481-13486.

Kerr, S. C., Azzouz, N., Fuchs, S. M., Collart, M. A., Strahl, B. D., Corbett, A. H.and Laribee, R. N. (2011). The Ccr4-Not complex interacts with the mRNA export machinery. PLoS One, *6*, e18302.

Kim, J. H., Choi, H. J., Kim, B., Kim, M. H., Lee, J. M., Kim, I. S., Lee, M. H., Choi, S. J., Kim, K. I., Kim, S. I., et al. (2006). Roles of sumoylation of a reptin chromatin-remodelling complex in cancer metastasis. Nat Cell Biol, *8*, 631-639.

Kim, J. H., Lee, J. M., Nam, H. J., Choi, H. J., Yang, J. W., Lee, J. S., Kim, M. H., Kim, S. I., Chung, C. H., Kim, K. I., et al. (2007). SUMOylation of pontin chromatin-remodeling complex reveals a signal integration code in prostate cancer cells. Proc Natl Acad Sci U S A, *104*, 20793-20798.

Kim, Y. W., Grossmann, T. N.and Verdine, G. L. (2011). Synthesis of all-hydrocarbon stapled alpha-helical peptides by ring-closing olefin metathesis. Nat Protoc, *6*, 761-771.

Kowalczyk, A. P., Bornslaeger, E. A., Borgwardt, J. E., Palka, H. L., Dhaliwal, A. S., Corcoran, C. M., Denning, M. F.and Green, K. J. (1997). The amino-terminal domain of desmoplakin binds to plakoglobin and clusters desmosomal cadherin-plakoglobin complexes. J Cell Biol, *139*, 773-784.

Krois, A. S., Ferreon, J. C., Martinez-Yamout, M. A., Dyson, H. J.and Wright, P. E. (2016). Recognition of the disordered p53 transactivation domain by the transcriptional adapter zinc finger domains of CREB-binding protein. Proc Natl Acad Sci U S A, *113*, E1853-1862.

Lanier, M., Schade, D., Willems, E., Tsuda, M., Spiering, S., Kalisiak, J., Mercola, M.and Cashman, J. R. (2012). Wnt inhibition correlates with human embryonic stem cell cardiomyogenesis: a structure-activity relationship study based on inhibitors for the Wnt response. J Med Chem, *55*, 697-708.

Lee, J. S.and Tung, C. H. (2010). Lipo-oligoarginines as effective delivery vectors to promote cellular uptake. Mol Biosyst, *6*, 2049-2055.

Lee, Y. H.and Stallcup, M. R. (2006). Interplay of Fli-I and FLAP1 for regulation of beta-catenin dependent transcription. Nucleic Acids Res, *34*, 5052-5059.

Li, L., Vorobyov, I.and Allen, T. W. (2013). The different interactions of lysine and arginine side chains with lipid membranes. J Phys Chem B, *117*, 11906-11920.

Li, Y., Bavarva, J. H., Wang, Z., Guo, J., Qian, C., Thibodeau, S. N., Golemis, E. A.and Liu, W. (2011). HEF1, a novel target of Wnt signaling, promotes colonic cell migration and cancer progression. Oncogene, *30*, 2633-2643.

Liu, J., Pan, S., Hsieh, M. H., Ng, N., Sun, F., Wang, T., Kasibhatla, S., Schuller, A. G., Li, A. G., Cheng, D., et al. (2013). Targeting Wnt-driven cancer through the inhibition of Porcupine by LGK974. Proc Natl Acad Sci U S A, *110*, 20224-20229.

Low, T. Y., Peng, M., Magliozzi, R., Mohammed, S., Guardavaccaro, D.and Heck, A. J. (2014). A systems-wide screen identifies substrates of the SCFbetaTrCP ubiquitin ligase. Sci Signal, *7*, rs8.

Madan, B., Ke, Z., Harmston, N., Ho, S. Y., Frois, A. O., Alam, J., Jeyaraj, D. A., Pendharkar, V., Ghosh, K., Virshup, I. H., et al. (2016). Wnt addiction of genetically defined cancers reversed by PORCN inhibition. Oncogene, *35*, 2197-2207.

Mae, M., El Andaloussi, S., Lundin, P., Oskolkov, N., Johansson, H. J., Guterstam, P.and Langel, U. (2009). A stearylated CPP for delivery of splice correcting oligonucleotides using a non-covalent co-incubation strategy. J Control Release, *134*, 221-227.

Miller, J. E.and Reese, J. C. (2012). Ccr4-Not complex: the control freak of eukaryotic cells. Crit Rev Biochem Mol Biol, *47*, 315-333.

Moellering, R. E., Cornejo, M., Davis, T. N., Del Bianco, C., Aster, J. C., Blacklow, S. C., Kung, A. L., Gilliland, D. G., Verdine, G. L.and Bradner, J. E. (2009). Direct inhibition of the NOTCH transcription factor complex. Nature, *462*, 182-188.

Morris, M. C., Gros, E., Aldrian-Herrada, G., Choob, M., Archdeacon, J., Heitz, F.and Divita, G. (2007). A non-covalent peptide-based carrier for in vivo delivery of DNA mimics. Nucleic Acids Res, *35*, e49.

Mosimann, C., Hausmann, G.and Basler, K. (2009). Beta-catenin hits chromatin: regulation of Wnt target gene activation. Nat Rev Mol Cell Biol, *10*, 276-286.

Muller, M. F., Ibrahim, A. E.and Arends, M. J. (2016). Molecular pathological classification of colorectal cancer. Virchows Arch, *469*, 125-134.

Nelson, A. R., Borland, L., Allbritton, N. L.and Sims, C. E. (2007). Myristoyl-based transport of peptides into living cells. Biochemistry, *46*, 14771-14781.

Newnham, L. E., Wright, M. J., Holdsworth, G., Kostarelos, K., Robinson, M. K., Rabbitts, T. H.and Lawson, A. D. (2015). Functional inhibition of beta-catenin-mediated Wnt signaling by intracellular VHH antibodies. MAbs, *7*, 180-191.

Nischan, N., Herce, H. D., Natale, F., Bohlke, N., Budisa, N., Cardoso, M. C.and Hackenberger, C. P. (2015). Covalent attachment of cyclic TAT peptides to GFP results in protein delivery into live cells with immediate bioavailability. Angew Chem Int Ed Engl, *54*, 1950-1953.

Oh, D., Nasrolahi Shirazi, A., Northup, K., Sullivan, B., Tiwari, R. K., Bisoffi, M.and Parang, K. (2014). Enhanced cellular uptake of short polyarginine peptides through fatty acylation and cyclization. Mol Pharm, *11*, 2845-2854.

Pelay-Gimeno, M., Glas, A., Koch, O.and Grossmann, T. N. (2015). Structure-Based Design of Inhibitors of Protein-Protein Interactions: Mimicking Peptide Binding Epitopes. Angew Chem Int Ed Engl, *54*, 8896-8927.

Persson, S., Killian, J. A.and Lindblom, G. (1998). Molecular ordering of interfacially localized tryptophan analogs in ester- and ether-lipid bilayers studied by 2H-NMR. Biophys J, *75*, 1365-1371.

Pokutta, S.and Weis, W. I. (2000). Structure of the dimerization and beta-catenin-binding region of alpha-catenin. Mol Cell, *5*, 533-543.

Polakis, P. (2012). Wnt signaling in cancer. Cold Spring Harb Perspect Biol, *4*.

Proffitt, K. D., Madan, B., Ke, Z., Pendharkar, V., Ding, L., Lee, M. A., Hannoush, R. N.and Virshup, D. M. (2013). Pharmacological inhibition of the Wnt acyltransferase PORCN prevents growth of WNT-driven mammary cancer. Cancer Res, *73*, 502-507.

Qian, Z., Martyna, A., Hard, R. L., Wang, J., Appiah-Kubi, G., Coss, C., Phelps, M. A., Rossman, J. S.and Pei, D. (2016). Discovery and Mechanism of Highly Efficient Cyclic Cell-Penetrating Peptides. Biochemistry, *55*, 2601-2612.

Qvit, N., Rubin, S. J., Urban, T. J., Mochly-Rosen, D.and Gross, E. R. (2016). Peptidomimetic therapeutics: scientific approaches and opportunities. Drug Discov Today.

Ragin, A. D., Morgan, R. A.and Chmielewski, J. (2002). Cellular import mediated by nuclear localization signal Peptide sequences. Chem Biol, *9*, 943-948.

Regberg, J., Srimanee, A., Erlandsson, M., Sillard, R., Dobchev, D. A., Karelson, M.and Langel, U. (2014). Rational design of a series of novel amphipathic cell-penetrating peptides. Int J Pharm, *464*, 111-116.

Richard, J. P., Melikov, K., Vives, E., Ramos, C., Verbeure, B., Gait, M. J., Chernomordik, L. V.and Lebleu, B. (2003). Cell-penetrating peptides. A reevaluation of the mechanism of cellular uptake. J Biol Chem, *278*, 585-590.

Rydberg, H. A., Matson, M., Amand, H. L., Esbjorner, E. K.and Norden, B. (2012). Effects of tryptophan content and backbone spacing on the uptake efficiency of cell-penetrating peptides. Biochemistry, *51*, 5531-5539.

Sack, U., Walther, W., Scudiero, D., Selby, M., Aumann, J., Lemos, C., Fichtner, I., Schlag, P. M., Shoemaker, R. H.and Stein, U. (2011). S100A4-induced cell motility and metastasis is restricted by the Wnt/β-catenin pathway inhibitor calcimycin in colon cancer cells. Mol Biol Cell, *22*, 3344-3354.

Sadot, E., Geiger, B., Oren, M.and Ben-Ze'ev, A. (2001). Down-regulation of beta-catenin by activated p53. Mol Cell Biol, *21*, 6768-6781.

Safholm, A., Tuomela, J., Rosenkvist, J., Dejmek, J., Harkonen, P.and Andersson, T. (2008). The Wnt-5a-derived hexapeptide Foxy-5 inhibits breast cancer metastasis in vivo by targeting cell motility. Clin Cancer Res, *14*, 6556-6563.

Sato, S., Idogawa, M., Honda, K., Fujii, G., Kawashima, H., Takekuma, K., Hoshika, A., Hirohashi, S.and Yamada, T. (2005). Beta-catenin interacts with the FUS proto-oncogene product and regulates pre-mRNA splicing. Gastroenterology, *129*, 1225-1236.

Sato, T., Van Es, J. H., Snippert, H. J., Stange, D. E., Vries, R. G., Van Den Born, M., Barker, N., Shroyer, N. F., Van De Wetering, M.and Clevers, H. (2011). Paneth cells constitute the niche for Lgr5 stem cells in intestinal crypts. Nature, *469*, 415-+.

Shitashige, M., Satow, R., Honda, K., Ono, M., Hirohashi, S.and Yamada, T. (2008). Regulation of Wnt signaling by the nuclear pore complex. Gastroenterology, *134*, 1961-1971, 1971 e1961-1964.

Takada, K., Zhu, D., Bird, G. H., Sukhdeo, K., Zhao, J. J., Mani, M., Lemieux, M., Carrasco, D. E., Ryan, J., Horst, D., et al. (2012). Targeted disruption of the BCL9/beta-catenin complex inhibits oncogenic Wnt signaling. Sci Transl Med, *4*, 148ra117.

Thorne, C. A., Hanson, A. J., Schneider, J., Tahinci, E., Orton, D., Cselenyi, C. S., Jernigan, K. K., Meyers, K. C., Hang, B. I., Waterson, A. G., et al. (2010). Small-molecule inhibition of Wnt signaling through activation of casein kinase 1alpha. Nat Chem Biol, *6*, 829-836.

Tian, Q., Feetham, M. C., Tao, W. A., He, X. C., Li, L., Aebersold, R.and Hood, L. (2004). Proteomic analysis identifies that 14-3-3zeta interacts with beta-catenin and facilitates its activation by Akt. Proc Natl Acad Sci U S A, *101*, 15370-15375.

Tyanova, S., Temu, T., Sinitcyn, P., Carlson, A., Hein, M. Y., Geiger, T., Mann, M.and Cox, J. (2016). The Perseus computational platform for comprehensive analysis of (prote)omics data. Nat Methods, *13*, 731-740.

Upadhyaya, P., Qian, Z., Selner, N. G., Clippinger, S. R., Wu, Z., Briesewitz, R.and Pei, D. (2015). Inhibition of Ras signaling by blocking Ras-effector interactions with cyclic peptides. Angew Chem Int Ed Engl, *54***,** 7602-7606.

Waaler, J., Machon, O., Tumova, L., Dinh, H., Korinek, V., Wilson, S. R., Paulsen, J. E., Pedersen, N. M., Eide, T. J., Machonova, O., et al. (2012). A novel tankyrase inhibitor decreases canonical Wnt signaling in colon carcinoma cells and reduces tumor growth in conditional APC mutant mice. Cancer Res, *72***,** 2822-2832.

Wender, P. A., Galliher, W. C., Goun, E. A., Jones, L. R.and Pillow, T. H. (2008). The design of guanidinium-rich transporters and their internalization mechanisms. Adv Drug Deliv Rev, *60***,** 452-472.

Wender, P. A., Mitchell, D. J., Pattabiraman, K., Pelkey, E. T., Steinman, L.and Rothbard, J. B. (2000). The design, synthesis, and evaluation of molecules that enable or enhance cellular uptake: Peptoid molecular transporters. P Natl Acad Sci USA, *97***,** 13003-13008.

Wexselblatt, E., Esko, J. D.and Tor, Y. (2014). On guanidinium and cellular uptake. J Org Chem, *79***,** 6766-6774.

Xu, W., Lau, Y. H., Fischer, G., Tan, Y. S., Chattopadhyay, A., De La Roche, M., Hyvonen, M., Verma, C., Spring, D. R.and Itzhaki, L. S. (2017). Macrocyclized Extended Peptides: Inhibiting the Substrate-Recognition Domain of Tankyrase. J Am Chem Soc, *139***,** 2245-2256.

Ziegler, A. (2008). Thermodynamic studies and binding mechanisms of cell-penetrating peptides with lipids and glycosaminoglycans. Adv Drug Deliv Rev, *60***,** 580-597.

## STAR METHODS

### KEY RESOURCES TABLE

See attached document.

### CONTACT FOR REAGENT AND RESOURCE SHARING

Further information and requests for resources and reagents should be directed to and will be fulfilled by the Lead Contact, Tom N. Grossmann (t.n.grossmann@vu.nl).

### EXPERIMENTAL MODEL AND SUBJECT DETAILS

#### Bacterial Strains

For expression of human full-length β-catenin *Escherichia coli (E. coli)* strain BL21-GOLD(DE3) was used and cultured in TB medium.

#### Cell Lines

The cell lines SW-480 and 293T were obtained from Deutsche Sammlung von Mikroorganismen und Zellkulturen (DSMZ) and the DLD-1 cell lines was purchased from the American Type Culture Collection (ATCC). HeLa, U87, MCF-7 and U2OS cell lines were kindly provided by Max Planck Institute of Molecular Physiology, Dortmund, Germany. Hek293T, HeLa, U87, MCF-7, U2OS were cultured in DMEM supplemented with 10% fetal calf serum, stable L-glutamine and 1x non-essential amino acids). DLD-1 and SW-480 were maintained in RPMI-1640 supplemented with 10% fetal calf serum and L-glutamine. Cultures were maintained at 37 °C in a humidified atmosphere of 5% CO2.

#### Mice

The Tet-O-β-catenin line mice had both the Tet-O-β-catenin allele and the ROSA26-M2-rtTA allele and were a mixed SV129 x C57Bl/6 background (Jarde et al. 2013). The small intestinal organoids used for the assays were obtained from a 4-month old male. The colony was bred and maintained in compliance with the UK's Animal (Scientific Procedures) Act under project license 30/3279 in filter top cages in a specific pathogen free facility under 12 h light/12 h dark conditions. Water and food were provided *ad libitum*.

### METHOD DETAILS

#### Peptide Synthesis

Peptides were synthesized following standard Fmoc-protocols for solid-phase peptide synthesis (Kim et al. 2011). Abbreviations for used chemicals can be found in Table S1. Peptide synthesis was performed on Rink

amide NovaSyn®TGR (Merck) or ChemMatrix® resin (Sigma-Aldrich). Amino acids were dissolved in DMF including 0.5 M OxymaPure® and coupled twice or three times. For coupling, amino acids were mixed with 3.9 eq of HCTU and 8 eq of DIPEA in DMF and added to the resin for 40 min. After amino acid coupling, the remaining free amino groups were blocked with NMP/acetic anhydride/DIPEA (10/1/1) for 2 min. Fmoc-deprotection was performed with 25 % piperidine in NMP for 10 min.

Crosslinking of unnatural olefinic amino acids (Okeanos Tech) was performed by ring closing metathesis (RCM). The dried resin was swollen in DCE for 30 min. A solution of Grubbs 1$^{st}$ generation catalyst (4 mg·mL$^{-1}$) in DCE was added to the resin and reacted for 1 h at room temperature. During reaction, nitrogen was bubbled through the mixture. The procedure was repeated five times and the resin was washed in a DMSO/DCM (1/1) solution for 10 min followed by a washing step in DCM.

To obtain a free N-terminus, peptides were deprotected with 25 % piperidine in NMP for 10 min. For acetylation, the last Fmoc-protecting group was removed and the free N-terminus was reacted twice with capping solution. Lipid and spermine modification were obtained through coupling of 4 eq of hexanoic acid, hexadecanoic acid or FBBSuc-OH using 3.9 eq PyBOP and 8 eq DIPEA. Fmoc-O2Oc-OH was coupled as a spacer to peptides subjected to FITC or NLS modification. FITC-labelling was performed twice with a 4-fold excess of FITC and 8 eq. DIPEA in NMP for 1 h. NLS was coupled according to the general SPPS protocol. Before biotinylation, Fmoc-NH-PEG(5)-COOH was introduced N-terminally using 3.9 eq PyBOP and 8 eq DIPEA. D-Biotin was coupled twice using PyBOP and DIPEA.

Peptides were cleaved from the resin with TFA/$H_2O$/TIPS (95/2.5/2.5) for 4 h and precipitated with diethyl ether at -20°C. Semi preparative HPLC was carried out on a LC-8A system (Shimadzu) using a Nucleodur C18 reverse-phase column (10 x 125 mm, particle size 5 µm, Macherey-Nagel; solvent A: water + 0.1 % TFA; solvent B: acetonitrile + 0.1 % TFA; flow rate: 6 mL·min$^{-1}$). Products were characterized on an analytical 1260 Infinity HPLC/ESI system (Agilent Technologies) equipped with a Zorbax C18 reverse-phase column (4.6 x 150 mm, particle size 5 µm, Agilent Technologies; solvent A: water + 0.1 % TFA; solvent B: acetonitrile + 0.1 % TFA; flow rate: 1 mL·min$^{-1}$). High-resolution mass spectra were recorded on a QLT Orbitrap mass spectrometer coupled to an Accela HPLC-System (HPLC column: Hypersyl GOLD, 50 mm x 1 mm particle size 1.9 µm, ionization method: Electrospray Ionization). Analytical data are shown in Supporting Table S2. According to Lambert-Beer law, yields were quantified by UV absorbance at 280 nm with an extinction coefficient of 11,000 M$^{-1}$·cm$^{-1}$ (StAx) or 5,500 M$^{-1}$·cm$^{-1}$ (StCo). FITC-labeled peptides were measured at

495 nm in 100 mM sodium phosphate buffer (pH 8.5) and calculated with an extinction coefficient of 77.000 $M^{-1} \cdot cm^{-1}$.

**β-catenin Expression and Purification**

*E. coli* BL21-Gold(DE3) cells (Agilent Technologies) were transformed with a modified pET-28a(+) plasmid engineered to harbour a C-terminal hexahistidine-tag and PreScission cleavage site after the full-length β-catenin gene. The gene coding for the full-length β-catenin protein is based on Genbank entry NM_001904.3. The fragment was obtained through gene synthesis (Integrated DNA Technologies). TB medium was inoculated with an overnight culture and incubated at 37° C until it reached an optical density of 1 at a wavelength of 600 nm. Protein expression was induced with 0.4 mM IPTG and incubated overnight at 18 °C. The harvested cell pellet was resuspended in a lysis buffer containing 50 mM Tris pH8.0, 300 mM NaCl, 1 mM β-mercaptoethanol, 5 % glycerol and cOmplete™, EDTA-free Protease Inhibitor Cocktail (Roche) and disrupted with a microfluidizer. Cell debris was removed through centrifugation at 70.000 rcf, 4 °C for 40 min. β-catenin was isolated from the lysate by affinity chromatography (His Trap™ HP, GE Healthcare). The N-terminal His-tag was not cleaved. The protein was eluted with an imidazole containing buffer (50 mM Tris pH8.0, 300 mM NaCl, 1 mM β-mercaptoethanol, 5 % glycerol and 250 mM imidazole). Further impurities were removed through size exclusion chromatography (20 mM Tris pH 8.0, 150 mM NaCl, 5 mM β-mercaptoethanol, 10 % glycerol; Column: HiLoad 16/600 Superdex 200, GE Healthcare). The protein solution was concentrated by ultrafiltration and was always used fresh in experiments.

**Fluorescence Polarization Assay**

β-Catenin was serially diluted in black, small volume, flat-bottom, non-binding 384-well plates (Greiner) in size exclusion buffer containing 0.05 % Tween 20 (FP buffer). 0.1 mM DMSO stock solutions of FITC-labeled peptides were dissolved in FP buffer to a 40 nM solution. Diluted peptides were then added to the protein and give a final concentration of 10 nM. After incubation for 1 h at 4 °C, the increase in fluorescence polarization of the fluorescently labeled ligand was recorded (Safire2, Tecan) with λ(ex) = 470 nm and λ(em) = 525 nm. $K_d$-values were determined by nonlinear regression analysis of dose-response curves (four parameters, variable slope) using GraphPad Prism 5 software (version 5.03).

**Flow Cytometry**

$5x10^4$ HeLa cells were plated in 24-well plates and allowed to grow 24 h in complete growth medium (DMEM supplemented with 10 % fetal calf serum, L-glutamine and non-essential amino acids). DMEM was carefully aspirated and cells were treated with fresh pre-warmed complete growth medium supplemented with 5 µM of peptide at a final concentration of 0.5 % DMSO or vehicle control only. After 90 min incubation, cells were

washed three times in PBS and treated for 3 min with 0.25% Trypsin/0.02% EDTA in PBS solution (PAN Biotech). The dissociation reaction was stopped using complete growth medium. Cells were then harvested through centrifugation (3 min, 180 g) and washed additional three times in PBS. Cells were then resuspended in 500 µL PBS and strained through a cell strainer cap into a 5 mL round-bottom tube (Falcon). Cells were subjected to a LSRII flow cytometer (BD). Using forward and side scattered light, a gate for intact, non-aggregated cells was defined. To obtain a statistical relevant population, the fluorescence at 530 nm of 10,000 events was collected within this cell gate (filter: 530/30, mirror: 502 LP). Data was analyzed using FlowJo software (version 10.1) and results were shown as geometric means of fluorescence collected at 530 nm.

**Confocal Microscopy**

$1.5x10^5$ HeLa cells were plated on 35 mm glass bottom dishes (MatTek) and cultured for 24 h in complete growth medium (DMEM supplemented with 10 % fetal calf serum, L-glutamine and non-essential amino acids). Then, DMEM was carefully aspirated and cells were treated with fresh pre-warmed complete growth medium supplemented with 5 µM peptide at a final concentration of 0.5 % DMSO or DMSO vehicle control. After 90 min treatment, cells were washed three times in warm PBS to remove excess peptide from the cell surface and left in pre-warmed imaging medium (PAN Biotech). Cells were immediately analyzed under a LSM510 meta confocal microscope (Zeiss) in a pre-warmed incubation chamber (37°C). By scanning through the z-planes of each cell, the outer plasma membrane borders were determined. Images were taken between the plasma membrane z-planes to obtain signals from internalized peptides and to minimize artificial signals from cell surface adhered peptides. Fluorescence was excited using a 488 nm argon laser (filter:505-540 BP). The distribution of FITC-labeled peptides was analyzed using a 63x Plan-Apochromat oil objective (Zeiss).

**Dual Luciferase Reporter Gene Assay**

Inhibitory potency of StAx peptides was tested with 293T cells in a 96-well format Wnt3a/β-catenin luciferase reporter gene assay (Lanier et al. 2012). HEK293T cells were cultured in DMEM supplemented with 10 % FCS at 37 °C in 5 % $CO_2$. For transient transfection, Lipofectamine®2000 (Thermo Fisher) and the appropriated plasmids were pre-incubated in Opti-MEM® medium for 15 min at room temperature. To cover a 96-well plate, $3x10^6$ cells were transiently transfected with Wnt3A-expressing vector for pathway activation, together with the commercially available Super(8x)TOPflash reporter vector harboring a (7×)TCF-firefly luciferase response element and the TK-driven Renilla luciferase co-reporter vector, as an internal transfection control to normalize the luminescence, and again incubated at 37 °C in 5 % $CO_2$ . After 8 h, cells

were harvested and counted. 25,000 transfected cells were seeded in 110 µL Media per well. Cells were allowed to adhere for 1 h. Cells were treated either with 10 µL of peptide solutions in different concentrations (final concentration 10, 5, 2.5, 1, 0.5, 0.25, 0.1 µM with 0.5 % DMSO), untreated and DMSO (0.5 %)-treated negative vehicle controls. After 22 h incubation, the medium was carefully aspirated. According to the manufacturer's protocol, cells were then lysed in lysis buffer followed by the addition of luciferase substrates from the Dual Glo®Luciferase Assay System (Promega). The quantitation of the stable luminescent signals of both *firefly* and *Renilla* luciferase was detected with a Tecan-Infinite 200 Plate Reader. Data was processed by normalizing *firefly* luciferase signal with *Renilla* luciferase signal from each well. Each condition was repeated as technical triplicate and the whole experiment were performed as independent biological replicates. The percentages of β-catenin-dependent canonical Wnt pathway inhibition by StAx-peptides were calculated with the GraphPad Prism 5 software (version 5.03). For calculation of $IC_{50}$-values (Figure S2), non-linear regression analysis (four parameters, variable slope) was performed.

**Pull-Down Assay**

10 cm dishes from adherent DLD-1 cells (70-80% confluency) were lysed in 200 µL lysis buffer (20 mM HEPES pH 7.5, 10 mM KCl, 1 mM $MgCl_2$, 1 mM $Na_2EDTA$, 1 mM EGTA, and 1x Halt™ Protease Inhibitor Cocktail (ThermoFisher Scientific) by four freeze-thaw cycles in liquid nitrogen, followed by sonication. Cell debris was removed by centrifugation for 20 min, 10,000 g, 4 °C, and protein concentration of the supernatant was measured using Bradford-Reagent (Serva). The lysate was diluted in binding buffer (50 mM TRIS pH 8.0, 300 mM NaCl) to 1 mg/mL. Dynabeads® M-280 Streptavidin (ThermoFisher Scientific) with a loading capacity of 200 pmol·$mg^{-1}$ were saturated with biotinylated *b*-StAx-h peptide for 1 h at room temperature on a rotating wheel. After washing three times in binding buffer, the beads were incubated with 1 mL cell lysate for 3 h at 4 °C on a rotating wheel. As a background control, Streptavidin beads alone were used. After washing the samples three times in binding buffer, samples were subjected to quantitative mass spectrometry.

**Mass Spectrometry of Pull-Down Assay**

Three replicates of peptide and control pull-downs were measured to obtain reliable label-free quantitative data. Before injection, samples were reduced, alkylated and digested directly on beads with LysC/Trypsin as previously described (Hubner et al. 2011). Obtained peptides were separated with a PepMap100 RSLC C18 nano-HPLC column (2, 100, 75 IDx25 cm, nanoViper, Dionex, Germany) on an UltiMate™ 3000 RSLCnano system (ThermoFisher Scientific) using a 125 min gradient from 5-60% acetonitrile with 0.1% formic acid and then directly sprayed *via* a nano-electrospray source (Nanospray Flex Ion Scource, Thermo Scientific) in a Q

Exactive™ Plus Hybrid Quadrupole-Orbitrap Mass Spectrometer (ThermoFisher Scientific). The Q Exactive™ Plus was operated in a data-dependent mode acquiring one survey scan and subsequently ten MS/MS scans. Resulting raw files were processed with the MaxQuant software (version 1.5.2.18) searching against an uniprot human database (ref. Jan 2016) using deamidation (NQ), oxidation (M) and acetylation (N-terminus) as variable modifications and carbamidomethylation (C) as fixed modification (Cox et al. 2008). A false discovery rate cut off of 1% was applied at the peptide and protein level. The integrated label-free algorithm was used for relative quantification of the identified proteins (Cox et al. 2014). Quantified proteins were further analyzed with Perseus (version 1.5.5.5) (Tyanova et al. 2016). Potential candidates interacting with *b*-StAx-h were required to be quantified in all three replicates (missing control values were imputated at the lower end of the distribution of all measured and quantified proteins) and were then identified with a two sample t-test. The result was visualized with a volcano plot (cut-off: p-value 0.01; S0 8).

**qRT-PCR from Small Intestinal Crypt Organoids**

Tet-O–β-catenin intestinal organoid culture was carried out as previously described (Sato et al. 2011):

The small intestine was dissected and washed internally with cold PBS, then cut longitudinally. The villi were then scraped off prior to the intestine being cut into small pieces and washed copiously in PBS. The epithelial tissue layer fragments were released from the underlying mesenchyme and smooth muscle, following chelation in 2 mM EDTA/PBS under agitation at 4°C, by repeated washes and agitation in PBS to collect the fragments. The pooled fragments were centrifuged (500 g, 5 min), strained through 70 µm mesh (Greiner) and centrifuged again (250 g, 5 min). Crypt structures were seeded in Matrigel (Corning) at a density of 100-200·50 $\mu L^{-1}$ and grown in Advanced DMEM (Invitrogen) supplemented with 1x B27, 1x N2, Penicillin/Streptomycin, 0.2% Fungizone, 1x Glutamax, 10 mM final concentration HEPES (all Invitrogen), 50 $ng \cdot mL^{-1}$ EGF (Sigma), 100 $ng \cdot mL^{-1}$ Noggin (Peprotech) and 400 $ng \cdot mL^{-1}$ R-spondin-1 (Peprotech). Structures start to bud after 2 days and were passaged every 7-10 days. Crypt structures were passaged by mechanical agitation in a 1 mL pipette tip, followed by centrifugation (250 g, 5 min) and seeding in fresh Matrigel (Jarde et al. 2013). Organoid cultures were routinely tested for mycoplasma (Lonza Myco Alert PLUS) and were found to be negative. Passage numbers 6-9 were used for drug assays. Crypt organoids were exposed to 4 $\mu g \cdot mL^{-1}$ doxycycline (dox) for 72 h; peptides were added to the medium for the last 2, 6, 10 or 24 h of the time course (final concentration 10 µM). The control treatment was exposure to dox for the whole time course of the experiment (in total 72 h). A dox withdrawal control was set up to make sure expression of Wnt responsive genes is dox-dependent. Organoids were exposed to 4 $\mu g \cdot mL^{-1}$ dox for 48 h. Then organoids were then placed in dox-free medium and cultured for additional 24 h. Dox withdrawal over 24 h stops

expression of ΔN-β-catenin and the consequent expression of Wnt responsive genes. The endpoint was qRT-PCR of Wnt response biomarkers Axin2, Myc, Ascl2, Tiam1 and the Wnt pathway repressed differentiation marker Car4. Intestinal crypt structures were lysed in 800 µL Trizol (Invitrogen) per 50 µL Matrigel blob of crypt organoids for RNA purification followed by 0.2 mg (per 50 µL Matrigel blob) of the RNA co-precipitant glycogen (Ambion, 5 $mg \cdot mL^{-1}$ stock). Chloroform/isoamyl alcohol mixture (Sigma) was added at 20 % Trizol volume to separate organic and aqueous layers and RNA was precipitated from the aqueous layer with 1 volume isopropanol and centrifuged (12,000 g, 20 min) and the pellet washed 2x in 75% ethanol. DNA was removed using the Turbo DNase kit (Ambion) using the manufacturer's instructions. The reverse transcription reaction was carried out using the Improm II kit (Promega) on 700 ng RNA. Analysis with qRT-PCR was carried out using the SensiFAST Sybr Hi-Rox 2x master mix (Bioline) using the manufacturer-recommended cycling protocol. Details of primers used for qRT-PCR can be found in **Fehler! Verweisquelle konnte nicht gefunden werden.**. Relative expression values were calculated using the $\Delta\Delta C_T$ method.

**Viability Assay**

For CellTiter-Glo® Assay, ca. 5,000 cells were plated in 96-well plates (Corning) 24 h prior to assay start. Then, medium was carefully aspirated and cells were treated with fresh pre-warmed complete growth medium supplemented with varying peptide concentrations (0.5-10 µM peptide at a final concentration of 0.5 % DMSO) or DMSO vehicle control only for 72 h. According to manufacturer's instructions, plates and reagents were equilibrated to room-temperature before one volume of CellTiter-Glo® reagent (Promega) was added to each well. For cell lysis, plates were shaken for 2 min on an orbital shaker. In order to obtain a stable signal, luminescence was recorded 10 min after reagent addition using a microplate reader (Safire2, Tecan).

**Wound-Closure Assay**

DLD-1 and MCF-7 cells were grown to confluence in 96-well ImageLock™ plates (Essen Biosciences) in complete growth medium. Wounds were generated with a WoundMaker™ device creating a homogenous 700-800 µm scratch. Growth medium was then aspirated and cells were then washed twice with PBS, and treated with complete media supplemented with DMSO vehicle control or 10 µM peptides until the scratch wound was closed. Photographs were taken with IncuCyte® Zoom Live-Cell Analysis System (Essen Biosciences). The percentage of wound closure was calculated with IncuCyte® Zoom Software (Essen Biosciences) by measuring the width unoccupied by cells, and normalized to the zero time point.

**QUANTIFICATION AND STATISTICAL ANALYSIS**

All data fitting and statistical analysis were performed using GraphPad Prism version 5.03 for Windows, GraphPad Software, La Jolla, California USA, www.graphpad.com. Statistical values including the exact n and statistical significance are also reported in the figure legends. For qRT-PCR on crypt organoids, viability and wound-closure assays, statistical significance was defined as $p \leq 0.05$ and determined by one-way ANOVA with Bonferroni's Multiple Comparison Test. Details on statistical analysis of the pull-down assay are explained in the corresponding STAR Methods section.